
**STATE RESEARCH CENTER OF RUSSIA**

**INSTITUTE FOR HIGH ENERGY PHYSICS**

IHEP 99-65

M.I.Barnik, S.G.Yudin
*Institute of Crystallography, Moscow*

V.G.Vasil'chenko*, S.V.Golovkin, A.M.Medvedkov
*Institute for High Energy Physics, Protvino*

A.S.Solovjev
*Joint Institute for Nuclear Research, Dubna*

# NEW SCINTILLATING MEDIA BASED ON LIQUID CRYSTALS FOR PARTICLES DETECTORS

Corresponding author. Fax: +7 7095 2302 337; e-mail: vasilchenko@mx.ihep.su

Protvino 1999

UDK 539.1.074.3 M–24

**Abstract**

Barnik M.I. et al. New Scintillating Media Based on Liquid Crystals for Particles Detectors: IHEP Preprint 99-65. – Protvino, 1999. – p. 10, figs. 9, refs.: 12.

The study results of optical, photoluminiscent and scintillation properties of a liquid crystal 4-pentyl-4′-cyanobiphenyl are presented. The scintillation light output of this liquid crystal is about 35% of crystal anthracene, main decay time constants are 4 ns and 14 ns and the maximum of light emission spectrum is about 400 nm. The light output of a dissolution of green emitting light scintillation dopant R6 in the liquid crystal is about 120% of crystal anthracene. The light output of the frozen dissolution measured at -112$^o$C is about 2.5 times higher as observed at +20$^o$C. In the uniaxially oriented liquid crystal, the predominant intensity direction of emitted light is pointed perpendicular to the liquid crystal director and an appreciable part of the emitted light is linearly polarized. A possibility to use scintillation properties of liquid crystals is considered both for the improvement of existing particles detectors characteristics and for the creation of new gated particles detectors.

**Аннотация**

Барник М.И. и др. Новые сцинтиллирующие среды на основе жидких кристаллов для детекторов частиц: Препринт ИФВЭ 99-65. – Протвино, 1999. – 10 с., 9 рис., библиогр.: 12.

В работе представлены результаты исследований оптических, фотолюминесцентных и сцинтилляционных характеристик жидкого кристалла 4-амил-4′-цианобифенил. Этот жидкий кристалл показал сцинтилляционный световыход около 35% от антрацена, времена высвечивания 4 и 14 нс и максимум спектра эмиссии около 400 нм. Световыход раствора жидкого кристалла и зеленой сцинтилляционной добавки R6 составляет около 120% от световыхода антрацена. Световыход этого замороженного раствора при -112$^o$C оказался в 2.5 раза выше его значений при +20$^o$C. Ориентированный жидкий кристалл обладает заметным уровнем поляризации излучаемого света. Максимальная интенсивность излучаемого света в ориентированном жидком кристалле направлена перпендикулярно к директору. Рассмотрены возможности использования жидких кристаллов как для улучшения характеристик существующих, так и для создания новых управляемых детекторов частиц.

## 1. Introduction

It is well known that a lot of liquid crystals (LCs) are derivatives of aromatic compounds. This is a reason for the study of their scintillation properties. LCs exhibit an anisotropy of their optical and luminescent properties which can be operated with the help of electrical and magnetic fields [1,2]. Due to the fact that LCs hold an intermediate position between organic solid crystals and isotropic liquids, it is expected that the efficiency of scintillators based on LCs can be higher than the best efficiency of ordinary liquid scintillators (LSs) based on isotropic liquids, and it can attain the efficiency of scintillators based on solid crystals (anthracene). These LCs scintillation properties can be used both for the improvement of existing particles detectors characteristics and for the creation of new gated particles detectors. This work is devoted to the study of scintillation properties of a LC that has demonstrated appreciable photoluminiscent properties in our preliminary investigations.

A temperature sensitive LC 4-pentyl-4′-cyanobiphenyl was chosen for our investigations. In the process of heating up from its solid crystal state, the LC phase transition temperatures are:

$$\text{solid crystal} \text{ — } +24^o\text{C} \text{ — NLC — } +35.1^o\text{C} \text{ — isotropic liquid,}$$

where NLC is the nematic texture of LC molecules. However, in the process of cooling from the isotropic liquid state, the LC retains its nematic texture in a temperature interval T = +35 – +15$^o$C, i.e. in this case the nematic texture of LC remains in a supercooled state in a temperature interval T = +24 – +15$^o$C. The LC density is 1.0065 g/cm$^3$ at T = +25$^o$C.

## 2. Measurement of optical and photoluminiscent characteristics

At first we carried out preliminary studies of some important optical and photoluminiscent characteristics of this LC for the above application. Different optical cells (OCs) filled with the LC were prepared for these measurements. Our OCs had the size

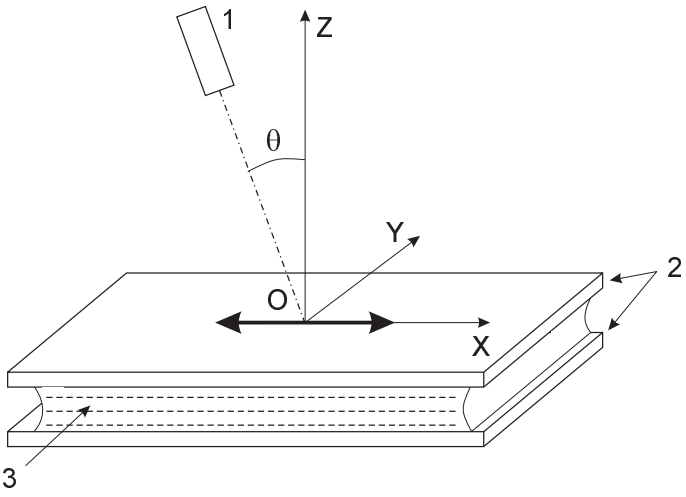


Fig. 1. Schematic view of our experimental setup: 1 — photomultiplier; 2 — quartz plates of optical cell; 3 — liquid crystal; ↔ — the direction of planarly orientated director of liquid crystal molecules.

of about 20×25 mm$^2$. The LC layers thicknesses in our OCs were chosen in an interval h = 30–200 $\mu$m. The schematic view of our experimental setup is illustrated in Fig.1. The conductive transparent coatings based on $SnO_2$ with thickness $< 0.1$ $\mu$m were evaporated onto the inner surfaces of some OCs quartz plates when the electrical field was supplied to these coatings to study its influence on the light output of these OCs. For aligning LC molecules in our OCs, the transparent thin films based on polyimides $< 0.1$ $\mu$m thick were also obtained on the inner plates surfaces (on $SnO_2$ coatings if they were used) [3]. In the absence of electrical field these films uniaxially oriented the LC director parallel to the X axis (Fig.1), i.e. they created the planar orientation of LC molecules in our OCs. For such LC orientation the predominant light emission intensity direction is expected to be pointed perpendicular to the OCs planes, i.e. parallel to the axis Z (Fig.1).

The LC photoluminescence was registered with the help of a photomultiplier (PM) that viewed the OCs from the same side they were excited by the UV light. While applying a certain value of the voltage to our OCs, the LC director swings to a maximum angle of about $90^o$ in the XZ plane (Fig.1), i.e. there occurs the LC reorientation in our OCs from the planar to gomeotropic texture where the LC director is perpendicular to the X axis. It is expected that an appreciable change (decrease) of the light output intensity detected by the PM should occur with the swing of LC director. This means that our OCs operate in a light valve mode under the application of electrical fields.

The LC absorption and photoluminiscent spectra are presented in Fig.2. As is clear from Fig.2 the maximum of light emission spectrum for the LC photoluminescence is about $\lambda_{em}$= 400 nm. The quantum efficiency $Y$ of the used PM is also presented in Fig.2. The optical transmission $Tr$ for some OCs with $SnO_2$ coatings is shown in Fig.3. The loss of light in these OCs was determined mainly by its absorption in $SnO_2$ coatings. The accuracy of $Tr$ measurements was about $\pm$ 1%.

At first the photoluminescence in OCs was excited by the isotropic (unpolarized) UV light with a wavelength $\lambda_{ex}$= 337 nm in order to investigate the light emission directionality from the oriented LCs. The fact that our OCs were excited by the isotropic light will be denoted in the text by the top index $i$ for the photoluminescence intensities $L$. When our OCs were excited by a planarly polarized light, i.e. when the LC director was in the same plane with the linearly polarized light, we used the top index $p$ for $L$. When

our OCs were excited by an orthogonally polarized light, i.e. when the plane of light polarization was perpendicular to the LC director, we used the top index $o$ for $L$. Similar designations we used in the text for the bottom indexes of $L$ in order to denote different types of polarized (or isotropic) light registered by the PM.

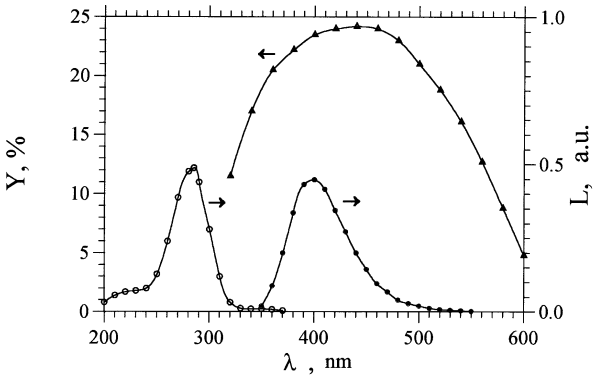


Fig. 2. Quantum efficiency of our photomultiplier $Y$ ($\triangle$), liquid crystal absorption ($\circ$) and photoluminescence spectra $L$ ($\bullet$) in chloroform ($\lambda_{ex}$= 320 nm) vs. the light wavelength $\lambda$. The curves were drawn to guide the eye.

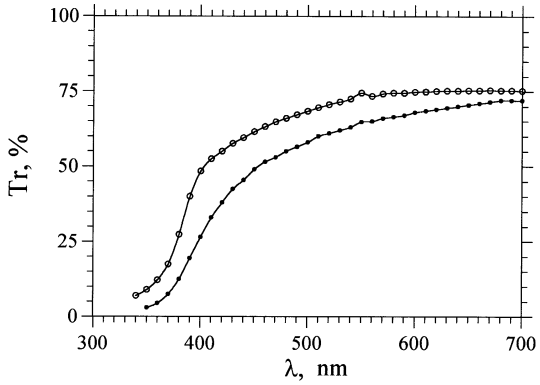


Fig. 3. Transmission spectra of used optical cells with $SnO_2$ claddings. $\circ$ — for h =30 $\mu$m, $\bullet$ — for h=200 $\mu$m.

Relative intensities and some polarization properties of the LC photoluminescence for an OC with h = 30 $\mu$m in the absence of electrical field have been measured. For this purpose we used film polarimeters placed directly before the PM or the OC. Note that our film polarimeters had a high level of transparency only for wavelengths $\lambda > 390$ nm. As a consequence, the LC scattered light influence (with $\lambda_{em}$= 337 nm) on the experimental results presented below was eliminated. Taking into account the planar symmetry of the LC director position in the OC, the measurements of photoluminescence intensities as a function of the viewing angle $\theta$ between a normal to the OC (the axis Z in Fig.1) and the direction of observation were carried out in an angle interval $0^o \leq \theta \leq 90^o$ in two mutually perpendicular planes. The accuracy of intensity measurements was about $\pm$ 5%.

The measurement results of the photoluminescence directionality of a planarly polarized light $L_p^i$ (i.e. $\theta$ is in the plane XZ Fig.1) are shown in Fig.4a and for an orthogonally polarized light – $L_o^i$ (i.e. $\theta$ is in the plane YZ) – in Fig.4b. As has been expected, the intensity of the planarly polarized part of photoluminescence is noticeably higher than that of the orthogonally polarized part of it. Therefore, the intensity of planarly polarized part of photoluminescence for an angle $\theta = 0^o$ is chosen as $L_p^i = 1$. So, the ratio of intensities of differently polarized parts of the photoluminescence for an angle $\theta = 0^o$ achieved a value of $L_o^i/L_p^i \simeq 0.40$. As might be expected, their angular distributions are close enough to each other.

Figs.4a-4b show that for that differently polarized parts of photoluminescence, the light emission intensity is predominantly directed perpendicular to the LC director. This

will allow us to gate the level of PM detected light intensity with the help of electrical field applied to OCs.

Measurements results of the directionality of photoluminescence excited by differently polarized light are presented in Figs.5a-5b. The emission intensity excited by the planarly polarized light $L_i^p$ is noticeably higher than the light intensity excited by the orthogonally polarized light $L_i^o$. Therefore, the emission intensity excited by the planarly polarized light is chosen as $L_i^p = 1$ for an angle $\theta = 0^o$. So, for the OC excited by differently polarized light, the ratio of their intensities is $L_i^o/L_i^p \simeq 0.38$ for $\theta = 0^o$. As might be expected, their angular distributions are close enough to each other.

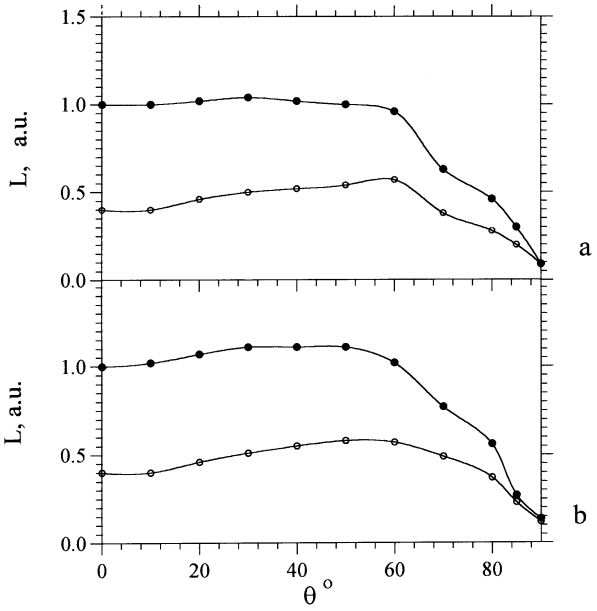


Fig. 4. Photoluminescence intensity $L$ for 30 $\mu$m optical cell vs. the viewing angle $\theta$. The cell was excited by isotropic light with $\lambda_{ex}$=337 nm. a) $\theta$ is in the plane XZ, b) $\theta$ is in the orthogonal plane YZ. PM detected different types of photoluminescence: for planarly polarized light (•) and for orthogonally polarized light (○). The curves were drawn to guide the eye.

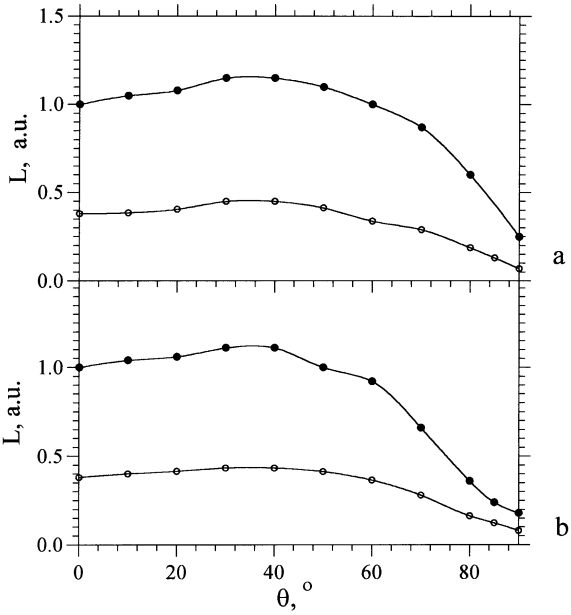


Fig. 5. Photoluminescence intensity $L$ for 30 $\mu$m optical cell vs. the viewing angle $\theta$. The cell was excited by polarized light with $\lambda_{ex}$=337 nm: for planarly polarized light (•) and for orthogonally polarized light (○). a) $\theta$ is in the plane XZ, b) $\theta$ is in the orthogonal plane YZ. PM detected the isotropic photoluminescence. The curves were drawn to guide the eye.

Fast changes of the directionality of photoluminescence intensity (note that the overall photoluminescence intensity in $4\pi$ angle remained at the same level) were observed with the application of electrical field to thin OCs. The measurements results of the excitation of OC with h = 30 $\mu$m by both the isotropic and polarized light having $\lambda_{ex}$= 337 nm and the application of electrical voltage are presented in

Fig.6. The threshold fall of photoluminescence intensity registered by the PM was observed for $U \geq 4$ V and $\theta = 0^o$. This fall was flattened out for $U \geq 8$ V. So, in a voltage interval 4.0 V $< U <$ 8.0 V the decrease of intensity was about two times. Note that the intensity of photoluminescence at the absence of electrical voltage was taken as 1.

The reaction time for a LC optical (and luminescent) characteristics with the application of electrical voltage to a OC is determined by expression [1]

$$t_1 = c_1 \eta h^2 / \varepsilon U^2, \qquad (1)$$

and the typical relaxation time for returning the above LC characteristics to their initial states after switching off the voltage is determined by expression [1]

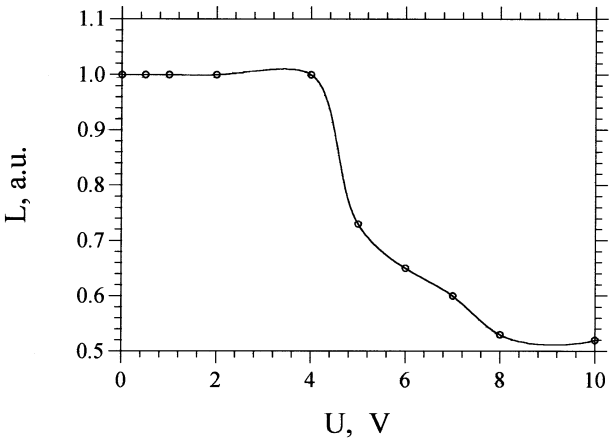


Fig. 6. Dependence of photoluminescence intensity $L$ for thin optical cell with h =30 $\mu$m vs. the applied voltage. The curve was drawn to guide the eye.

$$t_2 = c_2 \eta h^2 / k \qquad (2)$$

where $c_1$ and $c_2$ are some constants, $\eta$ is the viscosity of LC, $\varepsilon$ is the effective dielectric constant and $k$ is the elastic Frank constant of LC. So, a typical reaction time of our LC is $t_1 \simeq$0.8 s with the application of $U = 7$ V to an OC with h =30 $\mu$m and a typical relaxation time for our LC is about $t_2 \simeq 150$ ms. Formula (1) shows that in order to get LCs reaction time $t_1 \leq 1$ ms needed for high energy physics application, high voltage pulses should be applied to thin OCs filled with specially chosen LCs.

## 3. Measurement of scintillation characteristics

### 3.1. Measurement of light output

In order to measure the LC scintillation light output $I_o$, unoriented LC samples with the thickness of about h = 300 $\mu$m (and also the samples of another scintillator) were placed with an optical contact on the entrance window of PM FEU-84-3. This PM had a multialcali photocathode with the quantum efficiency $Y$ presented in Fig.2. The samples were excited with the help of a low intensity ($\sim 10^4$ Bk) radioactive source $^{241}$Am with the energy of $\gamma$-quanta of about 60 keV. Amplitude spectra both for our samples and crystal anthracene (with $\lambda_{em}$= 447 nm and h = 5 mm) were measured under the low energy $\gamma$-quanta excitation (in air, at room temperature). The position of edges of maximum amplitudes in these spectra approximately determined their relative light outputs $I_o$. The integration time of PM signals in these measurements was about 200 ns. The quantum efficiency of PM and the LC luminescent spectrum were taken into account at the determination of light output. The light output of anthracene was taken as 100%. The accuracy of light output determination by this method did not exceed $\pm$ 20%. Our

experience showed that this technique allowed us to determine the LC light output with an acceptable accuracy only for the samples with h $\geq$ 200 $\mu$m. Note that this technique may give a lowered level of light output values for organic scintillations in this energy region of $\gamma$-quanta. These lowered values might be caused by increased density of ionization along tracks of electrons knocked out by these low energy $\gamma$-quanta.

Another method [4] was used for the determination of light output temperature dependencies of samples scintillation $I$(T), because the above technique took a lot of time for the accumulation of necessary statistics during which the samples temperature in our setup significantly changed. According to the method there was no optical contact between the tested samples and PM entrance window because we did not manage to find any grease, which could provide it at a low temperature down to T = -120$^o$C. Scintillation in the tested samples was excited with the help of $\beta$-particles from radioactive source $^{90}$Sr + $^{90}$Y with an intensity of about $10^7$ Bk. The PM photocurrent was measured. The light output for these samples was normalized with the use of the above determined light outputs $I_o$.

Here the light output measurements were carried out in a temperature cycle in air. At first the samples were heated up +20$^o$C to +74$^o$C, then they were cooled down +74$^o$C to -112$^o$C, and again heated up -112$^o$C to +20$^o$C. The average rate of samples temperature changing in these measurements was made as slow as possible and achieved dT/dt $\leq$ 1$^o$C/min. The accuracy of relative light output determination in these measurements $I$ was about $\pm$5%.

However, this method of temperature light output determination for all samples suffers from an unavoidable, in such cases, drawback related to the fact that below the freezing temperatures, thin white layers of frozen LC and LS appear near the plates surfaces, probably, due to the appearance of multiple minicracks. Depending on their optical density, these layers may influence the measured levels of light outputs. So, they may enhance the level of frozen LC and LSs light outputs up to about 40%.

### 3.2. Measurement of decay times

The decay time constants $\tau$ of LC samples were measured by the single photoelectron delayed-coincidence counting technique [5] using PMs FEU-71 with quartz entrance windows. The scintillation in our LC and LSs was excited with the help of $\beta$-particles from a radioactive source $^{90}$Sr + $^{90}$Y. The time resolution of this experimental setup was about 0.5 ns. The measurement accuracy of decay times constants $\tau$ and their relative intensities A$_i$ did not exceed $\pm$ 6%. The experimental setup did not allow us to measure decay time constants with $\tau \geq$ 1000 ns.

## 4. Measurement results

A typical scintillation decay curve for the pure LC at T = +20$^o$C in air is presented in Fig.7 where N is counts per channel. The main decay times for this LC are $\tau_1$ = 4 ns, where A$_1$ $\simeq$53% from the total light output is emitted, and $\tau_2$=14 ns, where the rest A$_2$ $\simeq$47% is emitted. Note that unlike solvents in common LSs with $\tau$ = 30-60 ns [6], our pure LC shows components with short decay times.

The measurement results of amplitude spectra for the pure LC and crystal anthracene under the low energy $\gamma$-quanta excitation are presented in Fig.8a. The total absorption peak in the LC is less obvious under the low energy $\gamma$-quanta excitation, resulting from a smaller LC thickness in comparison with the used crystal anthracene. An approximate position of the total absorption peak in the pure LC is also shown in Fig.8a. Taking into account the PM quantum efficiency, the LC scintillation light output is $I_o \simeq 35\%$ under such low energy $\gamma$-quanta excitation.

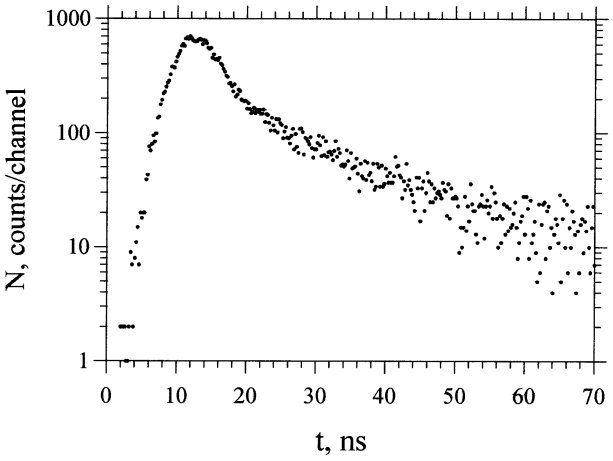


Fig. 7. A typical scintillation decay curve for pure liquid crystal.

Temperature dependencies of light outputs of the scintillation materials are important characteristic for numerous applications of LSs (especially in electromagnetic calorimeters, etc.). The measurement results of scintillation light output vs. the temperature for pure LC are presented in Fig.9a. It is clear from Fig.9a that after the temperature cycle of changes and returning it to T =+20$^o$C, the LC light output $I \simeq 29\%$ was in a good agreement with its value at T =+20$^o$C on the cooling curve and did not agree with the initial value $I_o \simeq 35\%$. However, at room temperature it took about 30 min for the LC light output to return to the initial value $I_o$.

It is obvious that there is a possibility to incorporate scintillation dopants into it and other LCs with the aim of further improvements of their scintillation characteristics. For this purpose a scintillation dopant R6[1] [7] (a pyrazoline derivative with $\lambda_{em}$= 490 nm and $\tau$ = 6.8 ns) was dissolved in the LC with a concentration of about 4 g/l. The measurement results of amplitude spectra for this dissolution and crystal anthracene under the low energy $\gamma$-quanta excitation are presented in Fig.8b. Taking into account the PM quantum efficiency to the R6 emission spectrum (a factor of $\simeq$ 1.28) [4], the light output of this dissolution is $I_o \simeq 120\%$. This experimental result confirms our above assumption of high efficiency of scintillators based on LCs (i.e. for those with the nematic texture).

The measurement results of scintillation light output vs. the temperature for the dissolution are presented in Fig.9b. It is clear from Figs.9a-9b, that their scintillation light outputs and temperature behaviours are alike. Sharp changes of the dissolution light output occur near the temperature of the LC texture transition from the nematic to isotropic liquid and vice versa at T$\simeq$+35$^o$C. High scintillation efficiency of the frozen dissolution draws our attention. So, the light output of the frozen dissolution is $I \simeq$305% at T = -112$^o$C. The nature of such enhanced level of the frozen dissolution light output is unknown to us yet. It is clear from Fig.9b that after the temperature cycle of changes and returning it to T = +20$^o$C, the dissolution light output $I \simeq 112\%$ was in a good agreement with its value at T = +20$^o$C on the cooling curve and did not agree with the initial value $I_o \simeq 120\%$. However, at room temperature it took about 30 min for the

[1]R6 is a trade mark of Geosphera Research Centre, Vavilova 70/2, Moscow, 117261 Russia.

dissolution light output to return to its initial value $I_o$. Note that optical and luminescent properties of dissolutions of LCs with scintillation dopants need a separate detailed study.

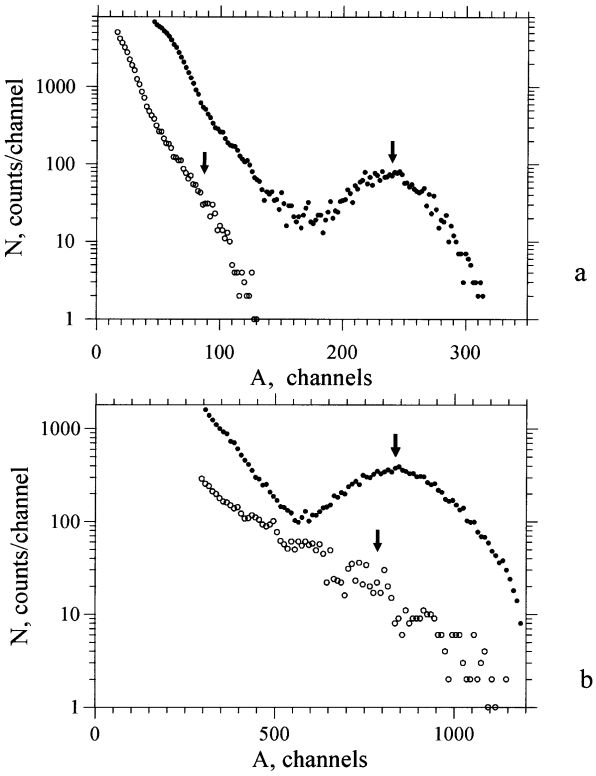


Fig. 8. Pulse height spectra of scintillation signals. a) — pure liquid crystal scintillation (o) and crystal anthracene (•); b) — liquid crystal dissolution with R6 scintillation dopant (○) and crystal anthracene (•). Samples were excited by $\gamma$-quanta from $^{241}$Am. Arrows show the location of total absorption peaks for 60 keV $\gamma$-quanta.

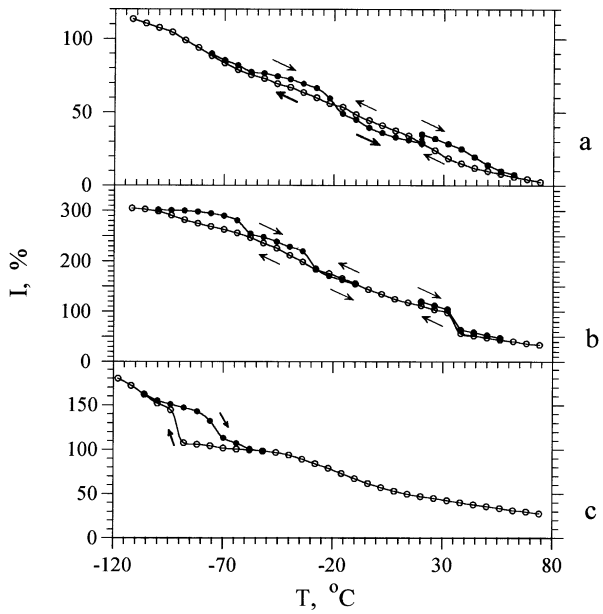


Fig. 9. Temperature dependencies of scintillation light outputs. a) — for pure liquid crystal; b) — liquid crystal solution with R6 scintillation dopant; c) — for BC-599-13G. (•) — for heating up and (○) — for cooling down. Arrows show sample temperature changes directions. When experimental data for heating up (dashed lines) and cooling down (solid line) processes agreed within measurements accuracy, only the data for cooling down process are presented.

The temperature dependence of light output for a well known LS based on monoisopropylbiphenyl BC-599-13G [8] with $\lambda_{em}$= 500 nm and $I_o \simeq 47\%$ is presented in Fig.9c for comparison. High scintillation efficiency of the frozen LS attracts our attention. So, the light output of frozen LS is $I \simeq 172\%$ at T = -112$^o$C and a tendency to its further increase has been observed with the temperature decrease. The nature of this effect is also unknown to us yet. Note that there are no considerable changes of the LC light output near the point of its phase transitions. Unlike the LS (Fig.9c and other experimental data on LSs presented in [4]) an additional loop of hysteresis of the LC light output is observed in its liquid states (Figs.9a-9b).

We explain such sharp changes of the LS light output (Fig.9c and other data also presented in [4]) at low temperatures by a process of the temperature polymorphism of

solid crystal structures for relatively simple organic compounds. So, the temperature transitions to some solid crystal structures are sometimes accompanied with the appearance of enhanced levels of the light output. These loops of hysteresis of light outputs can be related with the possibility of existence of some low temperature structures in solid crystals at higher temperatures.

With the application of voltage $U \geq 20$ V to a relatively thick OC with h = 100 $\mu$m, there was observed a change of the scintillation intensity $I$ only of $\simeq 9.5\%$. Additional measurements showed that with the application of the same voltage to the OC with h = 100 $\mu$m, there was observed a change of the photoluminescence intensity $L$ (both for the isotropic and polarized light with $\lambda_{ex}$= 337 nm) of $\simeq 11\%$. Note that these changes are comparable with each other. This points out that the LC optical valve mode of operation of the scintillation intensity can be carried out only for OCs with the thickness h $\leq 30$ $\mu$m.

Note that similar with the case of photoluminescence, the LC scintillation emission also showed a noticeable level of polarization. So, the ratio of the orthogonally polarized part of scintillation light to its planarly polarized part is $I_o/I_p \simeq 0.51$. However, the accuracy of these measurements was not better than $\pm$ 15%. Note that within the measurement accuracy, the ratio $I_o/I_p$ is close enough to the above determined ratio $L^i_o/L^i_p$.

## 5. Conclusion

The results of basic scintillation properties measurements for the liquid crystal 4-pentyl-4′-cyanobiphenyl are presented in here. So, this liquid crystal scintillation light output is about 35% of anthracene crystal and the light output of its dissolution with the green emitting light scintillation dopant R6 is about 120%, which is noticeably higher than the light output of commonly used liquid scintillators [8]. These levels of light outputs for the pure liquid crystal and its dissolution confirm our supposition of high efficiency for these new scintillation media.

Due to an acceptable level of transparency in the uniaxially oriented liquid crystal, a high level of the scintillation light output and its rather short decay times 4 and 14 ns, both pure liquid crystal and the dissolution show very promising possibilities of their applications in particles detectors. The above described design of the optical cells can be taken as a possible basis for the construction of particles detectors based on liquid crystals.

A search for other effective scintillation liquid crystals for particles detectors applications is desirable. However, such search for effective scintillation dopants for new media will require a long time. A more detailed research, which is beyond the aim of this paper, will be carried out in the near future.

The directionality of scintillation light emission in uniaxially oriented liquid crystals can also be exploited in particles detectors. So, we are going to use gomeotropically oriented liquid crystals with high refraction indexes in the tracking particles detectors based on capillary bundles [9] to increase the light output of capillaries.

The predominant intensity of both photoluminescence and scintillation emission in uniaxially oriented liquid crystal are directed perpendicular to the director and the emitted

light displays an appreciable level of linear polarization. It has been demonstrated that the intensity of emitted light from thin optical cells ($\leq$ 30 $\mu$m) can be effectively operated with the help of electrical field. This property can be used (as an alternative approach to that presented in [10,11]) in various devices, for example, in colour liquid crystal displays to increase their brightness. This can also be used for the creation of new gated particles detectors. However, the efficiency of scintillation light valve mode of operation in thin optical cells ($\leq$ 20-30 $\mu$m) based on liquid crystals needs a more accurate measurement.

The rise of light output for the frozen liquid crystal and its dissolution (as well as for some other frozen liquid scintillators presented in [4]) was observed with the decrease of temperature. Therefore, for T < -100$^o$C the light output of frozen dissolution exceeded the light output of crystal anthracene both for T = +20$^o$C and T = -70$^o$C [12]. Note that for a wide class of organic compounds their temperature behaviour of light output at lower temperatures (i.e. for T < -112$^o$C) and their ultimate values of light outputs (when the temperature approaches to T = -273$^o$C) need a more detailed study.

## Acknowledgements

The authors would like to express their deep gratitude to G.I.Britvich for his help in work and L.M.Blinov for his measurement of the luminescent spectra of liquid crystal.

## References

[1] A.P. Kapustin, "Experimental Investigations of Liquid Crystals", Nauka Publ., Moscow, 1978 (in Russian).

[2] S. Chandrasekhar, " Liquid Crystals ", Cambridge University Press Publ., Cambridge, 1977.

[3] M.I. Barnik et al., Molec. Mater. 6 (1996) 129.

[4] G.I. Britvich et al., Instrum. and Experim. Techn. v-41, No 1 (1998) 49.

[5] L.M. Bollinger, G.E. Thomos, Rev. Sci. Instrum. 32 (1962) 1044.

[6] I.B. Berlman, " Hand book of Fluorescence Spectra of Aromatic Molecules " Second edition, Academic Press, New York and London, 1971.

[7] V.G. Vasil'chenko et al., Instrum. and Experim. Techn. v-40 No 2 (1997) 175.

[8] Bicron Corporation, 12345 Kinsman Road, Newbery, Ohio 44065-9677, USA.

[9] N.S. Bamburov et al., Nucl. Instrum. and Methods. A 289 (1989) 265.

[10] Ch. Weder et al., Science 279 (1998) 835.

[11] A. Montali et al., Nature 392 (1998) 261.

[12] R.C. Saugster, M.I.T. Technical Report 1 (1952) 55.

*Received October 06, 1998*

М.И.Барник и др.
Новые сцинтиллирующие среды на основе жидких кристаллов для детекторов частиц.

Оригинал-макет подготовлен с помощью системы LaTeX.
Редактор Е.Н.Горина. Технический редактор Н.В.Орлова.

Подписано к печати 08.10.98. Формат 60 × 84/8. Офсетная печать.
Печ.л. 1.25. Уч.-изд.л. 0.96. Тираж 180. Заказ 37. Индекс 3649.
ЛР №020498 17.04.97.

ГНЦ РФ Институт физики высоких энергий
142284, Протвино Московской обл.

Индекс 3649

П Р Е П Р И Н Т 98-65, И Ф В Э, 1999